

Cite this: *Soft Matter*, 2011, **7**, 4101

www.rsc.org/softmatter

REVIEW

Viscoelasticity of the bacterial cell envelope

Virginia Vadillo-Rodríguez^a and John R. Dutcher^{*b}

Received 24th September 2010, Accepted 20th December 2010

DOI: 10.1039/c0sm01054e

Bacterial cell envelopes are remarkable biological structures that allow cells to adapt to and survive changes in their external environment while maintaining their mechanical integrity as the cells grow and divide. We review efforts to characterize the mechanical properties of the bacterial cell envelope, and we highlight recent advances in measurement techniques for individual bacterial cells that have led to a more complete understanding. In addition to their elastic behavior, bacterial cell walls also demonstrate a time dependent response to externally applied forces such that their mechanical properties are more properly described as viscoelastic. These measurements provide important information that is needed to understand the complex relationship between their structure and function.

Introduction

Microbial life has evolved over the last 3.6 billion years to withstand the many varied environments of the Earth's surface and subsurface, which include extremes in temperature, pH, pressure and salt concentration, as well as dramatic differences in the availability of food sources. In response to these challenges, bacteria have developed a wide range of sophisticated materials and mechanisms that allow the cells to move, grow and divide in different environments. One of their most remarkable structures is the bacterial cell envelope that serves as the interface between the cell and its external environment. The cell envelope incorporates a range of biological molecules in a sophisticated multilayer geometry which allows the maintenance of a positive turgor pressure between the inside and the outside of the cell, transport of nutrients into the cell and waste products out of the cell, and incorporation of special protein filaments such as flagella and pili, while also allowing the cell to grow and divide. Understanding the properties of the bacterial cell envelope provides a valuable insight into one of nature's most remarkable examples of nanotechnology. The present review discusses the previous work and recent advances in measurements of the mechanical properties of bacterial cells that have revealed the importance of time-dependent mechanical properties in accomplishing the ambitious goals that are necessary for the survival of bacteria.

Cell surface constituents and their structural organization

The bacterial cell envelope separates the contents of cells from their external environment, and its specialized properties

originate from the structural organization of three classes of macromolecules: polysaccharides, lipids and proteins. The different types of molecules self-assemble to form distinct layers that constitute the cell envelope. The fundamental difference in the organization of these layers accounts for the distinction between the two general classes of bacterial cells: Gram-positive and Gram-negative cells.^{1,2} In general terms, the cell envelope of Gram-positive cells consists of a relatively thick (20–80 nm) peptidoglycan layer that, together with the plasma membrane, sandwiches a viscous compartment called the periplasm, as shown schematically in Fig. 1.^{3,4} In contrast, the envelope of Gram-negative cells is made up of two lipid bilayers, the plasma membrane and the outer membrane, that are separated by a periplasm that contains a thin (3 to 8 nm thick) peptidoglycan layer, as shown schematically in Fig. 1.^{5,6}

The peptidoglycan layer is a covalently linked macromolecular structure that, as its name suggests, is made up of peptides and sugars. Its chemical composition is very similar in both Gram-positive and Gram-negative cells. The basic building block of the peptidoglycan consists of two sugar derivatives, *N*-acetylglucosamine and *N*-acetylmuramic acid, which are bonded together and to which are attached small linear peptide segments consisting of amino acids: L-alanine, D-alanine, D-glutamic acid and either lysine or diaminopimelic acid (Fig. 2a). The peptidoglycan building blocks are bonded together to form a three-dimensional network consisting of linear glycan chains that are joined by cross-links between the peptide segments. Further cross-linking occurs in Gram-negative cells by direct peptide linkage of the amino group diaminopimelic acid to the carboxyl group of the terminal D-alanine, whereas in Gram-positive cells cross-linking occurs mainly by peptide interbridges (Fig. 2b). Also found linked to or embedded in the peptidoglycan of Gram-positive cells are teichoic and lipoteichoic acids, the latter extending into the plasma membrane of the cells (see Fig. 1).⁷ Although the chemical constituents and assembly of the peptidoglycan components have been elucidated for some time, the nature of its

^aDepartment of Applied Physics, University of Extremadura, Badajoz, 06071, Spain

^bDepartment of Physics, University of Guelph, Guelph, Ontario, Canada N1G 2W1. E-mail: dutcher@uoguelph.ca; Fax: +1 519 836 9967; Tel: +1 519 824 4120 ext. 53950

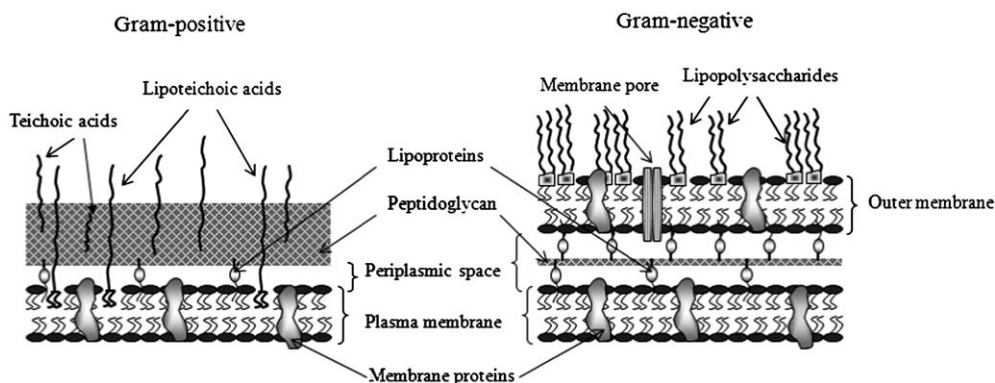


Fig. 1 Structural representation of the Gram-positive and Gram-negative cell envelopes. The Gram-positive cell envelope is composed of a thick peptidoglycan layer that lies outside the cytoplasmic membrane. Teichoic acids are linked to and embedded in the peptidoglycan, and lipoteichoic acids extend into the plasma membrane. The Gram-negative cell envelope is composed of an outer membrane linked by lipoproteins to a thin peptidoglycan layer, with an inner plasma membrane. The peptidoglycan layer is located within the periplasmic space that is created between the outer and inner membranes. The outer membrane includes porins, which allow the passage of small molecules across the membrane, and lipopolysaccharide molecules that extend into the extracellular space.

three-dimensional structure remains elusive. Two different models have been proposed to describe the higher order structure of the peptidoglycan: the traditional model, in which glycan strands are arranged parallel to the plasma membrane, primarily forming a single layer in Gram-negative cells and multiple crosslinked layers in Gram-positive cells, and the “scaffold model”, in which the glycan strands are postulated to lie perpendicular to the plasma membrane. Definitive evidence to support either of the two models is still missing.^{8,9}

Biological membranes consist primarily of proteins and amphipathic phospholipids. Phospholipids spontaneously arrange in aqueous solutions so that the hydrophobic fatty acid “tail” regions are shielded from the surrounding fluid, causing the more hydrophilic lipid “head” regions to associate with each other while remaining exposed to the aqueous environment.⁷ This forms a continuous lipid bilayer that, in the case of cell

membranes, includes inserted or associated proteins.^{10,11} Both the plasma and outer membranes of bacterial cells are lipid bilayers that contain proteins, but the outer membrane of Gram-negative cells also contains polysaccharides. Unlike the plasma membranes, the outer membrane of Gram-negative cells is highly asymmetric with the inner leaflet composed of phospholipids and the outer leaflet composed mostly of lipopolysaccharides (LPS) (Fig. 1).^{2,12} A LPS molecule is made up of two major regions: a polysaccharide region, which itself consists of two regions, the core oligosaccharide and the *O*-polysaccharide, and a lipid region, referred to as lipid A. The lipid A is not a glycerol lipid but a phosphorylated glucosamine disaccharide decorated with multiple fatty acids. These chains of fatty acids anchor the LPS molecule into the cell membrane and the rest of the molecule extends away from the cell surface.¹³ There are certain membrane proteins that form a unique chemical union between the outer

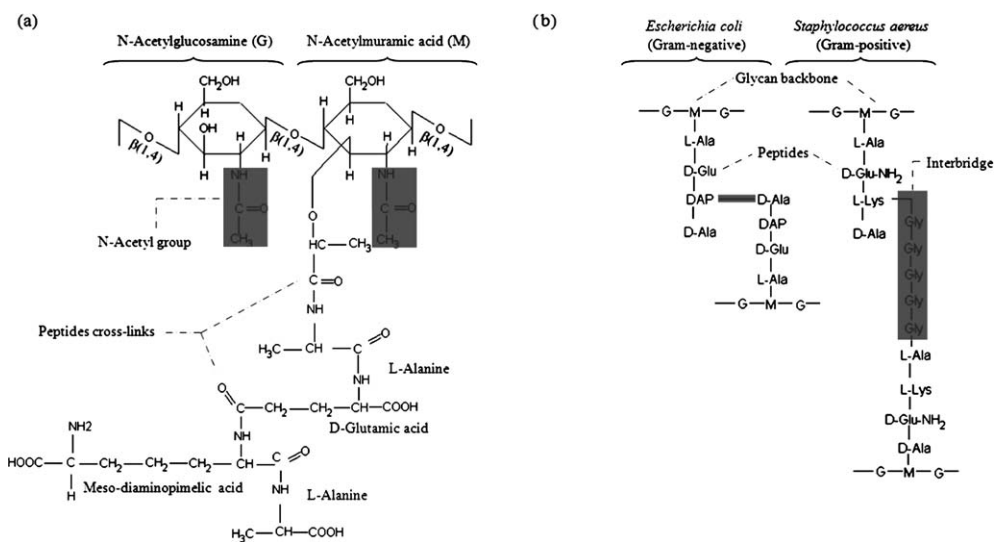


Fig. 2 Chemical structure of a glycan tetrapeptide (a) and the manner in which these molecules are connected (b) to form the peptidoglycan layer of *Escherichia coli* and *Staphylococcus aureus*, which are representative examples of Gram-negative and Gram-positive cells, respectively. The structure given in (a) corresponds to that found in *Escherichia coli*. Different bacterial species contain different amino acids.

membrane and the peptidoglycan layer of Gram-negative cells. These proteins, called lipoproteins, contain lipid tails that are deeply inserted into the hydrophobic domain of the membrane, with the “protein” portion linked to the peptidoglycan layer by either covalent or electrostatic bonds.^{1,14} Many other membrane proteins assemble into pores or channels allowing the passage of small molecules in and out the cells across their envelope.¹⁵

In nature, it is not unusual to find bacteria that also carry a variety of structures extending from their outer surface, such as fimbriae, pili and flagella, which are proteinaceous fiber-like appendages of variable length (0.2–10 μm) and width (7–20 nm), surface protein layers or S-layers consisting of a regular assembly of proteinaceous subunits that cover the cell, and capsules or slime layers, which are highly hydrated networks of polysaccharides extruded by the cells.^{16–18}

Mechanical role of the cell envelope

It is noteworthy that bacteria have been found living on Earth under a wide range of conditions: temperatures ranging from $-15\text{ }^{\circ}\text{C}$ to $121\text{ }^{\circ}\text{C}$, pH values ranging from 0.0 to 12.8, pressures ranging from atmospheric to those within the deep sea, and salt concentrations up to 30% [wt/vol] NaCl.^{19–22} Bacteria occur in many different shapes, ranging from spheres or ovoids (cocci), to cylinders (rods), to spirals (spirilla), to rings. Even square bacteria have been discovered in the extreme environment of saturated brine pools.²³ Despite the wide range of different shapes, bacteria share a common size which is typically on the micrometre scale. For example, rod-shaped bacteria such as *Escherichia coli*, *Pseudomonas aeruginosa* or *Bacillus subtilis* are typically several μm long and about $1\text{ }\mu\text{m}$ wide.^{24,25} Although the maintenance of nonspherical cell shapes is certainly largely accomplished by the mechanical strength of the peptidoglycan layer, the integrity of spherical cells also requires the reinforcement provided by the peptidoglycan layer. This realization arose from the observation that the chemical disruption of the peptidoglycan layer of rod-shaped bacteria results in the formation of spherical, osmotically sensitive, wall-less cells, whereas isolated, intact peptidoglycan from these cells retained the original rod shape of the intact cells.^{26,27} Ultra-thin sections of isolated walls visualized with cryo-transmission electron microscopy have also shown that the cellular shape retained by the wall of Gram-positive cells was lost after the extraction of teichoic acids.⁴ This finding highlighted the definitive role of teichoic acids in the maintenance of cell shape. Similarly, the nature of the bonding between the outer membrane and the peptidoglycan layer in Gram-negative cells through lipoproteins has been found to play a significant role in cell shape generation and/or preservation.²⁸

It is also important to note that the cell envelope is subjected to a significant osmotic or turgor pressure that is due to the large concentration of dissolved solutes inside the cell, *i.e.* salts, sugars, amino acids, vitamins, coenzymes, and a wide variety of other soluble materials that the cell needs to function properly. For Gram-negative cells grown under normal conditions, estimated values of the turgor pressure are in the range of 1–5 atmospheres (for reference, note that the pressure within an ordinary automobile tire is roughly 2 atmospheres), whereas for Gram-positive cells, the turgor pressure can be 20 to 50 atmospheres.^{29–32} It is the

cell envelope that protects the cells from swelling and bursting due to osmotic stress. Despite the presence of turgor pressure, the growth of rod-shaped cells does not occur uniformly in all directions. Instead, the rod-shaped cells elongate along the rod axis as they grow,⁷ revealing the anisotropic nature of the cell envelope.

A number of studies have also shown that forces acting on the cell surface can evoke responses at the level of gene expression. The marine bacterium *Vibrio parahaemolyticus*, for instance, responds to an increase in solution viscosity by turning on genes that lead to the production of lateral flagella that help the cells to propel themselves through the more viscous medium.³³ Adhesion of a cell to a solid surface leads to changes in genetic expression, characterizing the transition from planktonic to sessile states and signifying the shift toward the bacterial biofilm mode of operation.³⁴ It has also been found that genes can be both turned on and turned off in response to changes in environmental conditions such changes in pressure, temperature, pH and salt concentration.^{19,35–39} These results suggest that there is likely a corresponding change to the mechanical properties of the cell envelope produced by the transfer of information about the external environment into the cell.

From these previous studies, it is clear that the bacterial cell envelope plays a structural and protective role, and that understanding how this biological material interacts with and responds to its external environment requires, in addition to an understanding of its genetic regulation, detailed knowledge of its mechanical properties.

Time-dependent mechanical properties

Response of a viscoelastic solid material

In a soft or biological material in which there are both strong covalent bonds and other bonds that are relatively weak or transient, the application of an external force will generally result in a deformation of the material that varies with time. This response, which is referred to as a viscoelastic response, consists of both an instantaneous deformation, corresponding to a stretching of the strong bonds, and a deformation that increases with time, either continuously which corresponds to a flow of material (viscoelastic liquid) or as a deformation that approaches an asymptotic value (viscoelastic solid).⁴⁰ The measured response for a viscoelastic material depends on the time scale during which the external force is applied and during which the subsequent deformation is measured. Depending on the time scale and temperature of the experiment, a viscoelastic material can behave as an elastic solid, a viscous fluid, or as a combination of these two types of ideal materials.

For a viscoelastic solid material that is subjected to a constant external force, the time dependent deformation is referred to as creep.⁴¹ Creep deformation is typically associated with changes in the physical bonding interactions such as entanglements, van der Waals interactions and hydrogen bonding. The creep deformation occurs with a characteristic time scale that is determined by the viscoelastic properties of the material, and it can vary from molecular relaxation times of the order of picoseconds to “human” relaxation times of hours, days or even years.

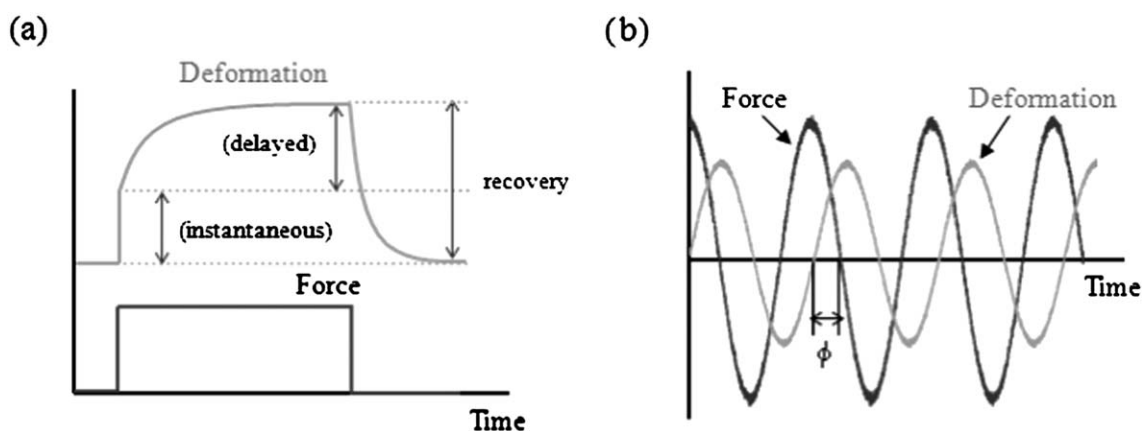


Fig. 3 Force and deformation as a function of time for a viscoelastic material subjected to (a) creep deformation and (b) dynamic testing. (a) In the idealized creep deformation experiment, a force is applied instantaneously to a viscoelastic solid; the force is held constant and the resulting deformation is recorded as a function of time. The material experiences an initial (instantaneous) elastic deformation followed by a time-dependent (delayed) elastic deformation that increases monotonically with time until it reaches an asymptotic value. After removal of the force, the material returns to its original undeformed state. (b) In the dynamic experiment, an alternating force is applied to the material and variations in its deformation (or force) are recorded as a function of time. The force and deformation both vary sinusoidally, with the deformation lagging the force by a phase lag of ϕ .

Measuring and modeling viscoelasticity

There are several classes of experiments that are used to measure the time-dependent mechanical properties of materials.⁴¹ Creep deformation measurements involve the rapid application of a force, which is then held constant as the resulting deformation is measured with time (see Fig. 3a). It is also possible to perform dynamic testing in which a sinusoidal force (or deformation) is imposed on the material and variations in its deformation (or force) are recorded as a function of time. The response of the material must also oscillate sinusoidally but it has, in general, a phase shift relative to the imposed force (or deformation) (see Fig. 3b).

The viscoelastic behavior that is inferred from these measurements is traditionally modeled using mechanical analogs that consist of a network of elastic springs and viscous dashpots.⁴⁰ Springs are used to represent the elastic response of the material, and dashpots (that can be thought of as oil-filled cylinders in which a loosely fitting piston moves at a rate proportional to the viscosity of the oil and the applied force) are used to describe the fluid behavior, or the removal and reestablishment of transient bonds. Viscoelastic phenomena such as creep deformation and stress relaxation have been described using spring-and-dashpot models for a wide variety of different materials, ranging from polymers^{40–43} to building materials⁴⁴ to biological materials.^{45–47}

As an example, a three-element mechanical model consisting of a spring (k_1) placed in series with a parallel arrangement of a spring (k_2) and a dashpot (η_2) is shown in Fig. 4. This model, known as the Standard Solid Model (SSM), describes a material that, in response to a constant force, experiences an instantaneous deformation and a subsequent deformation that gradually increases with time, asymptotically approaching a final value. The deformed material eventually completely relaxes to its original state after the loading force is removed (see Fig. 3a), and therefore does not involve flow of material.^{40,48} The spring element k_1 represents the initial (instantaneous elastic)

deformation. The latter time-dependent (delayed elastic) deformation is described by the delayed deformation experienced by the spring k_2 as determined by the viscosity η_2 that characterizes the dashpot element. The rate at which the delayed deformation occurs is typically expressed in terms of the so-called retardation or characteristic time τ , which is given by the ratio η_2/k_2 for this particular model. The rate at which the external force is applied and the characteristic time τ together define the extent of the distinctive hysteresis loop that viscoelastic materials exhibit in their force-deformation curves (the force is larger during the loading than during the unloading process).

Mechanical models such as the SSM are described by differential equations that can be used to predict the deformation of the material under investigation. These equations typically

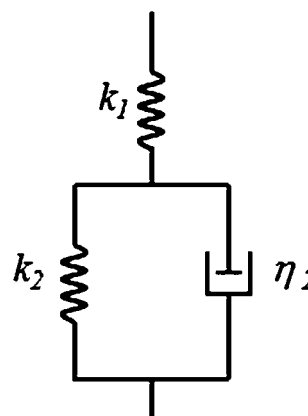


Fig. 4 A schematic diagram of a three-element mechanical model, known as the Standard Solid Model, is shown. It consists of an elastic spring with stiffness k_1 , which describes an instantaneous elastic deformation, in series with a parallel combination of a spring with stiffness k_2 and a dashpot with viscosity η_2 , which describes a delayed elastic deformation. This model has recently been used to characterize the viscoelastic behavior of bacterial cells.^{69–71}

involve the force (F), the deformation (X) and their derivatives with respect to time, as well as the elastic (k) and viscous (η) constants of the model. For the SSM, the governing differential equation can be expressed as:^{48,49}

$$\frac{dF(t)}{dt} + \frac{k_1 + k_2}{\eta_2} F(t) = k_1 \frac{dX(t)}{dt} + \frac{k_1 k_2}{\eta_2} X(t) \quad (1)$$

The solution to eqn (1) for a material subjected to a constant step force F_0 is of the form:

$$X(t) = \frac{F_0}{k_1} + \frac{F_0}{k_2} \left[1 - \exp\left(-t \frac{k_2}{\eta_2}\right) \right]. \quad (2)$$

If, instead, the material is exposed to a sinusoidal force $F(t) = F_0 \exp(i\omega t)$ (where ω is the angular frequency), the mechanical response determined by the solution to eqn (1) is complex, $E^*(\omega) = F(t)/X(t) = E_1(\omega) + iE_2(\omega)$, in which the real $E_1(\omega)$ and imaginary $E_2(\omega)$ parts that describe the time-dependent elastic and viscous response of the material are given by:

$$E_1(\omega) = \frac{\omega^2 \eta_2^2 k_1 + k_1 k_2 (k_1 + k_2)}{(k_1 + k_2)^2 + \omega^2 \eta_2^2} \quad (3)$$

$$E_2(\omega) = \frac{\omega \eta_2 k_1^2}{(k_1 + k_2)^2 + \omega^2 \eta_2^2} \quad (4)$$

Therefore, the time-dependent mechanical response of a material described by the SSM is characterized by the elastic parameters k_1 and k_2 and the viscosity parameter η_2 , which are obtained by fitting the corresponding experimental data to eqn (2)–(4).

Probing the mechanical properties of bacterial cells and their isolated surface layers

Early experimental observations

For many years, techniques for measuring the mechanical properties of bacterial cells did not exist and it was simply acknowledged that the strength of the bacterial cell wall was large enough to withstand the turgor pressure. The cell wall was also thought to be an inherently rigid structure given that vigorous physical methods were required to rupture cells and that the shape of isolated walls and wall fragments resembled that of intact cells.²⁹ However, in the late 1960s, Marquis surprisingly found that the Gram-positive *Bacillus megaterium* cells could contract as much as 26% (in terms of dextran-impermeable volume) in response to the environmental ionic strength and pH changes.⁵⁰ This contraction was reversible, and because it did not occur in sucrose solutions of equivalent osmolality, it was primarily attributed to electrostatic interactions within the peptidoglycan rather than to an osmotic response of the cells. Later, this hypothesis was experimentally supported by Koch and Woeste^{51,52} who combined manipulation of the net wall charge of Gram-negative *Escherichia coli* cells, by altering the pH of the suspending medium, with low-angle laser light-scattering measurements of the surface area of the cells. They determined that the isolated walls could reversibly expand up to 300% relative to their relaxed state, whereas the surface

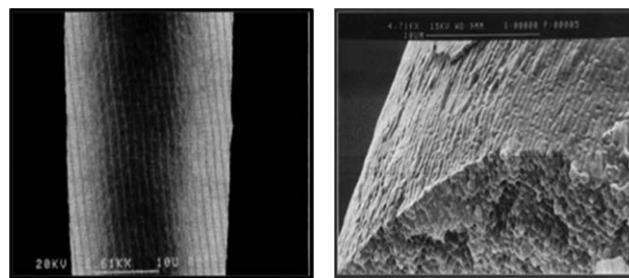


Fig. 5 Scanning electron micrographs showing the surface and a cross-section of a bacterial thread of a separation-suppressed mutant of *Bacillus subtilis*.^{54,55}

area of intact cells merely decreased by 20% once the cells were devoid of their internal pressure. Further compelling evidence demonstrating the flexibility of bacterial cells was presented by Isaac and Ware in 1974.⁵³ The authors embedded different types of bacterial cells in glycerol–gelatine strips and stretched them on a rack under the lens of a microscope. The *Spirillum* cells were found to uncoil and stretch reversibly to a rod three times the length of their original shape. The Gram-positive bacterium, *Bacillus megaterium*, was observed to elongate by one quarter of its original length before becoming detached from the gel matrix. *Escherichia coli* cells stretched up to 100% of their length without detaching from the gel. However, for the Gram-positive coccus, *Staphylococcus aureus*, no elongation was detected prior to detachment from the gel matrix. The apparent lack of flexibility of these latter cells was attributed to their thicker peptidoglycan layer.

In 1985, a more direct quantification of the mechanical properties of bacterial cells became possible with the study of bacterial threads. Thwaites and Mendelson presented a novel method to produce threads from multiple filaments of a separation-suppressed mutant of *Bacillus subtilis* (Fig. 5).⁵⁴ Surprisingly, the dimensions of these biological fibers (up to 1 m in length and 100 μm in diameter) allowed them to be studied using conventional textile engineering techniques. A series of experiments were performed that consisted of extending individual fibers at a constant speed while recording the force as a function of the extension. In a subsequent set of experiments, threads were redrawn from solutions of various pH and ionic strengths, and occasionally, from lysozyme solutions.⁵⁵ The experiments were performed in a controlled atmosphere enclosure, and the measured properties were extrapolated, based on a number of assumptions, to those of the cell wall. It was found that the cell wall became gradually more ductile as the salt concentration of the pre-suspending medium increased, whereas pre-treatment with lysozyme or variations in the pH of the pre-suspending medium did not significantly change the measured mechanical properties.⁵⁵ At low relative humidity, the cell wall generally acted as a glassy polymer, *i.e.* it was stiff, strong and brittle. However, at high relative humidity the cell wall became weaker, softer and ductile, with its behavior resembling that of a rubbery polymer. It was also reported that the cell wall mechanical properties depended on the speed of the applied extension, which is a distinctive characteristic of viscoelastic materials. In particular, cells were found to be stiffer and more brittle at higher extension rates.^{56,57} For the first time, the viscoelastic nature of the bacterial cell wall was beginning to be revealed

experimentally. Unfortunately, the difficulty in producing filament-forming mutant strains restricted the application of this methodology to *Bacillus subtilis* and no further studies were reported.

Direct measurements

Evaluation of the mechanical properties of individual bacterial cells, which was a long time challenge because of their small size, became possible in the mid-1990s with technical advances that provided the tools that are needed to control the local deformation of micron-sized objects with high spatial and force resolution. The first studies on the mechanical strength of single cells were carried out by Shiu *et al.*⁵⁸ In these experiments, individual Gram-positive and Gram-negative cells suspended in a drop of water were squeezed until rupture between a glass plate and a flat optical fiber connected to a force transducer, revealing bursting forces of 13.8 μN and 3.6 μN , respectively. When the cells were partially squeezed and the induced deformation maintained, the forces measured were found to relax with characteristic time constants that ranged between 0.6 and 1.6 s. This observation, which did not occur at the higher compression rate studied of 6.2 $\mu\text{m s}^{-1}$, was partially attributed to a possible viscoelastic response of the cells. Although these were remarkable measurements, the bursting force is not the most suitable parameter to describe the mechanical behavior of cells.

The elastic properties of single bacterial cells and cell components have also been determined using atomic force microscopy (AFM). In these measurements, a sharp tip (typical radius of curvature of 10 to 50 nm) at the free end of a flexible cantilever is commonly used to image the surface topography of the sample.^{59–72} Beveridge and co-workers pioneered the determination of quantitative mechanical data for bacterial surface materials using the AFM imaging mode.^{64,65} In particular, isolated bacterial membranes were deposited over solid supports containing narrow grooves and repeatedly imaged while increasing the imaging force. Cross-sections along the images revealed a marked depression of the membranes into each groove

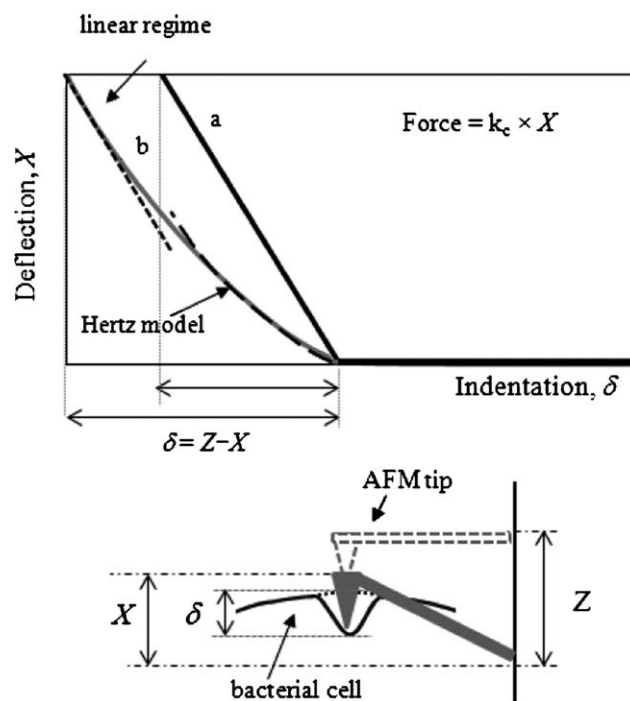


Fig. 6 Typical deflection of an AFM cantilever with a colloidal (curve a) and a pyramid-shaped (curve b) tip as it indents the surface of a bacterial cell. The mechanical response of the cell to indentation by a relatively large, colloidal tip (radius of 300 nm) is found to be linear. An effective cell spring constant is readily obtained from the force-indentation curve by calculating the ratio between the loading force and the depth of indentation. The cell response to a pyramid-shaped tip usually exhibits both nonlinear and linear regimes. The slope of the linear regime determines the spring constant of the cell. The nonlinear regime is generally fitted to the Hertz model, yielding the Young's modulus of the cell.

relative to the solid support. By relating the imaging force to the observed depression distances, the elastic properties of the suspended membranes were determined for the first time. Values of

Table 1 Collection of values reported in the literature for the spring constant K_1 and Young's modulus Y of Gram-negative and Gram-positive cells obtained from the analysis of AFM force-indentation curves

Strain	Spring constant K_1 (N m^{-1})	Young's modulus Y ($\times 10^6 \text{ N m}^{-2}$)	Ref.
Gram-negative			
<i>Magnetospirillum gryphiswaldense</i>	0.042–0.070 (in buffer)	—	66 and 67
<i>Sphingomonas paucimobilis</i>	—	0.05–0.08 (in GM ^a)	72
<i>Pseudomonas aeruginosa</i>	0.02–0.26 (in GM ^a and DI ^a water)	—	73
	0.044–0.11 (in DI ^a water)	—	69
<i>Escherichia coli</i>	0.037–0.19 (in buffer)	—	68
	0.026–0.078 (in DI ^a water)	—	70 and 75
	0.1–0.9 (in NaCl)	—	76
	—	182–221 (in air)	79
	—	1.9–6.1 (in buffer)	80
<i>Shewanella putrefaciens</i>	0.01–0.05 (in buffer)	0.037–0.21 (in buffer)	74
	0.064–0.129 (in buffer)	0.069	77 and 78
	0.061–0.088 (in buffer)	—	78
Gram-positive			
<i>Lactobacillus</i>	0.016–0.053 (in buffer)	—	81
<i>Staphylococcus aureus</i>	—	88–95 (in air)	79
	0.006–0.053 (in buffer)	0.189–1.764 (in buffer)	82
<i>Bacillus subtilis</i>	0.10 (in DI ^a water)	—	71

^a GM and DI stand for growth media and deionized water, respectively.

$\sim 3 \times 10^{10} \text{ N m}^{-2}$ and $3\text{--}4 \times 10^8 \text{ N m}^{-2}$ were determined for Young's modulus of the dried proteinaceous sheath of the archaeon *Methanospirillum hungatei* and the isolated peptidoglycan layer of Gram-negative cells, respectively. Shortly after these initial studies, the use of AFM tips as mechanical indenters emerged, which allowed the local measurement of the mechanical properties of micron-sized objects.^{66–68} This has led to the collection of force-indentation curves that are generated by simultaneously recording the cantilever deflection and the vertical movement of the z-piezoelectric transducer as the tip (or sample) approaches and pushes into the sample (or tip). The resulting cantilever deflection is directly related to the applied force *via* the spring constant of the cantilever, k_c . The indentation values are obtained by subtracting the vertical position of the z-piezoelectric transducer from the deflection of the cantilever as the tip (or sample) approaches and pushes onto the sample (or tip) (Fig. 6). For this analysis, it is assumed that the deflection of the cantilever during the approach of the AFM tip to the sample results exclusively from the mechanical indentation of the sample, and that other interactions between the tip and the sample (*e.g.* electrostatic forces) are not significant. For bacterial cells, which are less stiff than the cantilever, this assumption has been experimentally confirmed.⁶⁹ If the cell response to the loading force is linear, an effective cell spring constant can be readily obtained from force-indentation curves by calculating the ratio between the loading force and the depth of indentation (Fig. 6a, Table 1).^{66–70} Yet, more often than not, the approach portion of the force-indentation curves exhibits both nonlinear and linear regimes at low and high loading forces, respectively (Fig. 6a).^{72–82} The linear regime has been ascribed to the compression of the plasma membrane of the cell, with the slope corresponding to the value of the effective spring constant of the cell. Theoretical expressions have been derived to relate the measured cell compression and spring constant values to the turgor pressure of the cell, and reasonable values were obtained

for the turgor pressure of both Gram-negative and Gram-positive cells.^{67,83} Unfortunately, the calculations of the turgor pressure also require as input parameters the exact radius of the AFM tip and many other physical parameters that are difficult to know precisely. The nonlinear regime is usually analyzed according to the Hertzian theory of elastic deformations.^{72,74,77,79,80,82,84} This theory describes the indentation of a non-deformable indenter (the AFM tip) into an infinitely extending deformable elastic half space (a planar soft sample). The AFM tip geometry is generally approximated as either a conical or paraboloid indenter. For these cases, the functional relationships between the loading force (F) and the depth of indentation (δ) are given by⁸⁵

$$F_{\text{cone}} = \frac{2}{\pi} \frac{E}{1-\nu^2} \tan(\alpha) \delta^2 \quad (5)$$

$$F_{\text{paraboloid}} = \frac{4}{3} \frac{E}{1-\nu^2} R^2 \delta^{\frac{3}{2}} \quad (6)$$

where E and ν are, respectively, the surface elastic constant and the Poisson ratio of the material constituting the elastic half-space, α is the half-opening angle of a conical tip, and R is the radius of curvature of the paraboloid or spherical indenter. Fitting the nonlinear behavior of the force-indentation curves to eqn (5) and (6) has yielded values of Young's modulus that are of the order of 10^7 to 10^8 Pa for different bacterial strains (Table 1). However, inherent to the Hertz model is the assumption that the diameter of the contact area must be much smaller than the radius of the indenter.⁸⁴ It has recently been shown that this condition is rarely satisfied when bacterial cells are indented with standard (sharp) AFM tips.⁶⁹ To resolve this conflict, relatively large, colloidal AFM tips were used.

Although elastic constants have been the most commonly reported parameters to characterize the mechanical behavior of

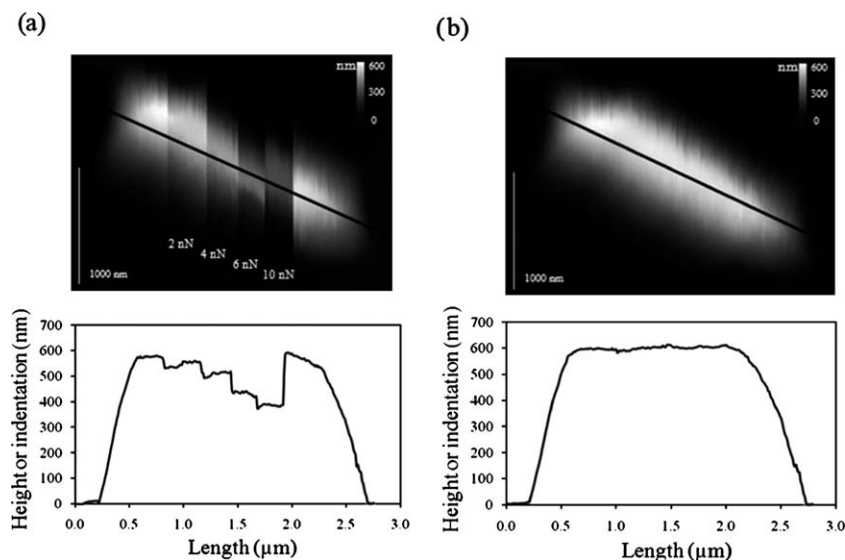


Fig. 7 AFM topographic images of an *Escherichia coli* (*lpp*⁺) cell obtained in contact mode using an AFM pyramid-shaped tip. (a) Image was collected by increasing the contact force in a stepwise fashion during the scan. The cross-section corresponds to the black line shown in the AFM image along the length of the cell. The indentations estimated from the AFM images under different loading force values have been shown to agree quantitatively with those measured from force-indentation curves. (b) Image collected after that shown in (a) using a small value of the contact force (1 nN).

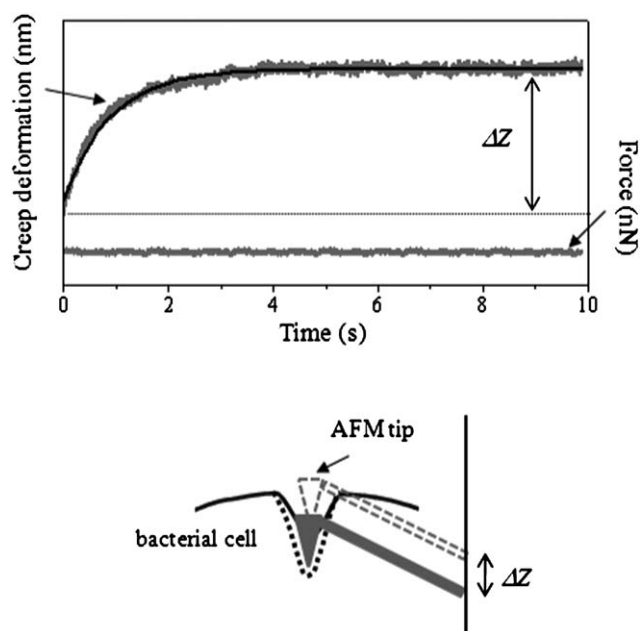


Fig. 8 Example of the creep deformation experienced by an *Escherichia coli* (*lpp*) bacterial cell when subjected to a constant force of 6 nN as a function of time. The force is applied with an AFM colloidal tip and maintained by keeping the cantilever deflection constant with time. The creep deformation corresponds to the indentation of the AFM tip into the cell with time. The total creep deformation ΔZ is ~ 10 nm for this particular example. The solid black line corresponds to the best fit of the data to eqn (2).

bacterial cells, they do not provide a complete description. Recently, we and our co-authors have used a new AFM technique to demonstrate that individual bacterial cells are not purely elastic, but have a mechanical response that is more properly described as viscoelastic.^{69–71} In these studies, a colloidal AFM tip (radius of 300 nm) was used to apply and maintain a constant force to fully hydrated individual bacterial cells. To achieve good reproducibility, cells were imaged using AFM and selected to be of typical dimensions (see Fig. 7), indicating that they were at the same stage of their growth cycle, and to be physically separated from neighbouring cells. By varying the applied force during AFM imaging, large deformations of the cell were observed, as shown in Fig. 7a. Subsequent imaging of the same cell using small contact forces revealed that the large deformations

previously induced by the larger loading forces were completely reversible with the cell wall still intact (Fig. 7b). For the measurement of the viscoelastic properties of the bacterial cells, the AFM tip was pressed onto the centre of the top of the bacterial cells. Following the rapid indentation of the AFM tip into the cells (Fig. 6), the tip further indented the cells with time until an asymptotic value was reached (Fig. 8), corresponding to a creep deformation of the bacterial cell envelope.^{69–71} In essence, this is a nanoscale version of a conventional creep experiment that is used to study the viscoelastic properties of bulk materials. The creep response of the cells, which was independent of the magnitude of the applied force, was analyzed in terms of the Standard Solid Model (SSM). In Fig. 8, the best fit of the data to eqn (2) is shown as a solid line. The best-fit viscoelastic parameters obtained in this manner for different bacterial strains are summarized in Table 2. The values given for each bacterial strain are averages of the values measured for a large number of cells, and the uncertainties quoted for each value are the standard deviations of the values measured for each bacterial strain. The relatively small uncertainties indicate that the AFM creep deformation experiment is a very well-defined and reproducible physical measurement for a wide range of bacterial strains. Both sharp and colloidal AFM tips were used in the experiments, with the use of colloidal tips ensuring a linear viscoelastic response.

The relative importance of the elastic and delayed elastic contributions to the mechanical response of the cells was found to depend on the specific composition and interactions between the molecules within the cell envelope and thus, clear differences between the mechanical properties of Gram-negative and Gram-positive cells were observed. For instance, the peptidoglycan layer has been shown to be quite elastic,^{50,52,65} a property that is mainly attributed to the flexibility of the peptide segments that cross-link the glycan chains. It is reasonable to assume that the elastic strength of the cells will depend on the thickness of the peptidoglycan layer, and in fact, the Gram-positive *B. subtilis* 168 strain was found to be less deformable than any of the Gram-negative strains (see Table 2). In addition, the differences found in the levels of deformability between *E. coli* (*lpp*⁺) and its *Lpp* mutant *E. coli* (*lpp*) further suggested that it is not only the thickness of the peptidoglycan layer, but also the bound form of the peptidoglycan–lipoprotein complex which contributes to the rigidity of the cell envelope.⁷⁰ The viscous response of the cells is related to a number of properties that affect the fluidity of the cell membranes, such as the length of the LPS molecules and the

Table 2 Summary of the viscoelastic parameters of bacterial cells studied using the AFM-based creep deformation experiment.^{69–71} These values were obtained from a least-squares fit of the AFM creep response of the cells to eqn (2) (Standard Solid Model). The parameters k_1 and k_2 are elastic stiffness values, η_2 is a viscosity value, and τ is the characteristic response time of the cells which is defined as the ratio η_2/k_2

	Viscoelastic parameters			
	k_1 (N m ⁻¹)	k_2 (N m ⁻¹)	η_2 (Ns m ⁻¹)	τ (s)
Gram-negative				
<i>Pseudomonas aeruginosa</i>	0.044 ± 0.002	0.81 ± 0.08	1.37 ± 0.27	1.82 ± 0.20
<i>P. aeruginosa</i> (GA-treated)	0.11 ± 0.03	1.5 ± 0.1	1.0 ± 0.2	0.8 ± 0.3
<i>Escherichia coli</i> K12	0.056 ± 0.008	0.54 ± 0.13	0.36 ± 0.05	0.64 ± 0.08
<i>Escherichia coli</i> (<i>lpp</i> ⁺)	0.045 ± 0.010	0.54 ± 0.10	0.61 ± 0.28	1.1 ± 0.2
<i>Escherichia coli</i> (<i>lpp</i>)	0.026 ± 0.006	0.33 ± 0.06	0.30 ± 0.07	0.91 ± 0.30
Gram-positive				
<i>Bacillus subtilis</i> 168	0.10 ± 0.02	1.2 ± 0.3	3.0 ± 0.6	2.6 ± 1.1

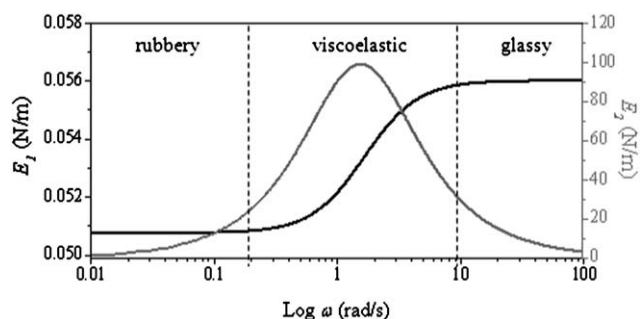


Fig. 9 Plot of the dynamic elastic E_1 and viscous E_2 response of an *Escherichia coli* K12 cell as a function of frequency. The curves represent the analytical solutions to the Standard Solid Model and were generated by substituting the cell viscoelastic parameters listed in Table 2 into eqn (3) and (4).

presence of stabilizing cations.⁷¹ Accordingly, the fluidity of the *P. aeruginosa* PAO1 membrane was expected to be lower than that of *E. coli* K12 and this is in agreement with the observations (Table 2). Therefore, collectively, the measured viscoelastic response of these cells, with surface layers that differ both chemically and structurally, suggested that their elasticity is dominated by the peptidoglycan layer and the nature of its association with the membranes, whereas the viscous component is more likely to arise from the liquid-like character of the membranes.^{70,71} Furthermore, the values of the viscoelastic parameters of the cells listed in Table 2 were substituted into eqn (3) and (4) to generate for the first time a full description of the elastic (E_1) and viscous (E_2) properties of the cells over a wide range of force loading rates (or, equivalently, a wide range of effective frequencies). Example calculated curves are shown in Fig. 9, and good agreement was obtained with experimental data.⁷¹ It was found that at low and high frequencies, the mechanical behavior of the cells is that of a rubbery and glassy material, respectively. In the intermediate frequency regime, which corresponds to time values that are comparable to the characteristic time τ of the cells, the mechanical behavior of the cells is consistent with the calculated viscoelastic response. Collectively, the results of the AFM-based creep deformation experiments indicate that Gram-negative and Gram-positive cells exhibit a viscoelastic solid-like character in response to an external force, with their mechanical response dependent on the rate at which the force is applied.

Biological significance of the viscoelastic behavior of bacterial cells

The viscoelastic nature of bacterial cells likely plays an important role in the life of the cells. For instance, as cells grow, it is necessary to break some of the bonds within the very thin, highly stressed peptidoglycan network so that new peptidoglycan material can be inserted. The breaking of bonds is accomplished by autolysin molecules that are produced within the cell and transported through the cell wall. Maintaining the mechanical integrity of the peptidoglycan layer during cell growth is a challenging requirement for the cell, since the breaking of a bond will transfer stress to neighboring bonds, which are consequently easier to break. This could lead to a “domino” type of reaction,

causing a tear or fissure and the eventual lysis of the cell. It is possible that the viscoelastic response of the bacterial cell wall, as observed in the creep deformation studies, could delay the accumulation of localized strain and allow bonds to reform before the rupture of the network can occur. This proposed mechanism for maintaining the peptidoglycan network integrity during hydrolase activity has the advantage that it does not require the existence of other specialized enzymes that have been postulated^{86,87} but have not been observed.

The viscoelastic properties of bacterial membranes also help to determine the proper structures and time scales within the bacterial cell membranes that are necessary for the transport of molecules into and out of the cells, which is typically mediated by membrane proteins. In addition, the design of novel, molecular-based antimicrobial strategies often involves targeting a desired change to the mechanical properties of the cell wall through association or insertion of molecules such as cationic antimicrobial peptides. Many more fundamental aspects of cell behavior are likely to be soon deciphered from an improved and integrated understanding of cell structure and mechanics.

Concluding remarks

Through adaptation and survival, bacterial cells have developed sophisticated structures of remarkable mechanical integrity from simple biological material components. Recent progress in experimental techniques provides unprecedented opportunities to probe the mechanical properties of individual bacterial cells, which have a complexity that is only now beginning to be understood. By applying and extending principles that have been developed for macroscopic studies of the mechanics of engineering materials, these measurements provide important information that is needed to establish linkages between structure, mechanical properties and function.

Acknowledgements

The authors gratefully acknowledge financial support from the Advanced Foods and Materials Network (AFMNet), the Canadian Foundation for Innovation and the Natural Sciences and Engineering Research Council of Canada. JRD acknowledges support from the Canada Research Chairs (CRC) program.

References

- 1 M. T. Cabeen and C. Jacobs-Wagner, *Nat. Rev. Microbiol.*, 2005, **3**, 601–610.
- 2 T. J. Beveridge, in *Bacteria in Nature*, ed. J. S. Poindexter and E. R. Leadbetter, 1989, vol. 3, pp. 1–65.
- 3 V. R. F. Matias and T. J. Beveridge, *J. Bacteriol.*, 2006, **188**, 1011–1021.
- 4 V. R. F. Matias and T. J. Beveridge, *Mol. Microbiol.*, 2005, **56**, 240–251.
- 5 A. Bernadac, M. Gavioli, J. C. Lazzaroni, S. Raina and R. Loubes, *J. Bacteriol.*, 1998, **180**, 4872–4878.
- 6 V. R. F. Matias, A. Al-Amoudi, J. Dubochet and T. J. Beveridge, *J. Bacteriol.*, 2003, **185**, 6112–6118.
- 7 M. T. Madigan, J. M. Marinko and J. Parker, in *Brock Biology of Microorganisms*, Prentice Hall, New York, 10th edn, 2003, ch. 4, pp. 55–81.
- 8 B. J. Dmitriev, F. V. Toukach, K.-J. Schaper, O. Holst, E. T. Rietschel and S. Ehlers, *J. Bacteriol.*, 2003, **185**, 3458–3468.

- 9 W. Vollmer and J.-V. Holtje, *J. Bacteriol.*, 2004, **186**, 5978–5987.
- 10 Y.-M. Zhang and C. O. Rock, *Nat. Rev. Microbiol.*, 2008, **6**, 222–233.
- 11 D. M. Morries and G. J. Jensen, *Annu. Rev. Biochem.*, 2008, **77**, 583–613.
- 12 N. Ruiz, D. Kahne and T. J. Silhavy, *Nat. Rev. Microbiol.*, 2006, **4**, 57–66.
- 13 H. Nikaido, *Microbiol. Mol. Biol. Rev.*, 2003, **67**, 593–656.
- 14 T. J. Beveridge, *Int. Rev. Cytol.*, 1981, **72**, 229–317.
- 15 R. E. W. Hancock, R. Siehnel and N. Martin, *Mol. Microbiol.*, 1990, **4**, 1069–1075.
- 16 P. S. Handley, *Biofouling*, 1990, **2**, 239–264.
- 17 H. J. Busscher, H. C. van der Mei and P. S. Handley, in *Physical Chemistry of Biological Interfaces*, ed. A. Baszkin and W. Norde, Marcel Dekker, New York, 2000, ch. 13, pp. 431–458.
- 18 U. B. Sleytr and P. Messner, *Annu. Rev. Microbiol.*, 1983, **37**, 311–339.
- 19 I. R. Booth, in *Biology of Prokaryotes*, ed. J. W. Lengeler, G. Drews and H. G. Schlegel, Thieme, New York, 1999, ch. 28, pp. 652–671.
- 20 R. Y. Morita, *Bacteriol. Rev.*, 1975, **39**, 144–167.
- 21 T. D. Brock, *Annu. Rev. Ecol. Syst.*, 1970, **1**, 191–220.
- 22 H. H. Zahran, *Biol. Fertil. Soils*, 1997, **25**, 211–223.
- 23 A. E. Walsby, *Nature*, 1980, **283**, 69–71.
- 24 R. A. Freitas and R. C. Merkle, in *Kinematic Self-Replicating Machines*, Landes Biocience, Texas, 2004, ch. 4, pp. 89–144.
- 25 L. M. Prescott, J. P. Harley and D. A. Klen, in *Microbiology*, William C. Brown Publishers, Iowa, 3rd edn, 1996, pp. 37–41.
- 26 J. Lederberg, *Proc. Natl. Acad. Sci. U. S. A.*, 1956, **42**, 574–577.
- 27 C. Weibull, *J. Bacteriol.*, 1953, **66**, 688–695.
- 28 I. Sonntag, H. Schwarz, Y. Hirota and U. Henning, *J. Bacteriol.*, 1978, **136**, 280–285.
- 29 R. J. Doyle and R. E. Marquis, *Trends Microbiol.*, 1994, **2**, 57–60.
- 30 A. M. Whatmore and R. H. Reed, *J. Gen. Microbiol.*, 1990, **136**, 2521–2526.
- 31 T. J. Beveridge, *Can. J. Microbiol.*, 1988, **34**, 363–372.
- 32 A. L. Koch, *Adv. Microb. Physiol.*, 1983, **24**, 301–366.
- 33 R. Belas, M. Simon and M. Silverman, *J. Bacteriol.*, 1986, **167**, 210–218.
- 34 P. Becker, W. Hufnagle, G. Peters and M. Herrmann, *Appl. Environ. Microbiol.*, 2001, **67**, 2958–2965.
- 35 L. N. Csonka, *Microbiol. Rev.*, 1989, **53**, 121–147.
- 36 D. Bartlett, M. Wright, A. A. Yayamos and M. Silverman, *Nature*, 1989, **342**, 572–574.
- 37 A. Stintzi, *J. Bacteriol.*, 2003, **185**, 2009–2016.
- 38 P. D. Cotter and C. Hill, *Microbiol. Mol. Biol. Rev.*, 2003, **67**, 429–453.
- 39 G. Jubelin, A. Vianney, C. Beloin, J.-M. Ghigo, J.-C. Lazzaroni, P. Lejeune and C. Dorel, *J. Bacteriol.*, 2005, **187**, 2038–2049.
- 40 I. M. Ward and D. W. Hadley, *An Introduction to the Mechanical Properties of Solid Polymers*, John Wiley & Sons, Hoboken, NJ, 1993.
- 41 J. D. Ferry, *Viscoelastic Properties of Polymers*, John Wiley & Sons, Hoboken, NJ, 3rd edn, 1980.
- 42 M. V. Voinova, M. Rohdahl, M. Jonson and B. Kasemo, *Phys. Scr.*, 1999, **59**, 391–396.
- 43 C. B. Roth, B. Deh, B. G. Nickel and J. R. Dutcher, *Phys. Rev. E: Stat., Nonlinear, Soft Matter Phys.*, 2005, **72**, 021802.
- 44 J. P. Wolf, *Earthquake. Eng. Struct. Dynam.*, 1997, **26**, 931–949.
- 45 M. Frisén, M. Mägi, L. Sonnerup and A. Viidik, *J. Biomech.*, 1969, **2**, 13–20.
- 46 B. W. Towler, C. J. Rupp, A. B. Cunningham and P. Stoodley, *Biofouling*, 2003, **19**, 279–285.
- 47 P. C. Y. Lau, J. R. Dutcher, T. J. Beveridge and J. S. Lam, *Biophys. J.*, 2009, **96**, 2935–2948.
- 48 W. N. Findley, J. S. Lai and K. Onaran, *Creep and Relaxation of Nonlinear Viscoelastic Materials with an Introduction to Linear Viscoelasticity*, Dover Publications, Inc., New York, NY, 1989.
- 49 M. Qaisar, *Pure Appl. Geophys.*, 1989, **131**, 703–713.
- 50 R. E. Marquis, *J. Bacteriol.*, 1968, **95**, 775–781.
- 51 A. L. Koch, *J. Bacteriol.*, 1984, **159**, 919–924.
- 52 A. L. Koch and S. Woeste, *J. Bacteriol.*, 1992, **174**, 4811–4819.
- 53 L. Isaac and G. C. Ware, *J. Appl. Microbiol.*, 1974, **37**, 335–339.
- 54 J. J. Thwaites and N. H. Mendelson, *Proc. Natl. Acad. Sci. U. S. A.*, 1985, **82**, 2163–2167.
- 55 J. J. Thwaites, U. C. Surana and A. M. Jones, *J. Bacteriol.*, 1991, **173**, 204–210.
- 56 J. J. Thwaites and N. H. Meldenson, *Int. J. Biol. Macromol.*, 1989, **11**, 201–206.
- 57 J. J. Thwaites and U. C. Surana, *J. Bacteriol.*, 1991, **173**, 197–203.
- 58 C. Shiu, Z. Zhang and C. R. Thomas, *Biotechnol. Tech.*, 1999, **13**, 707–713.
- 59 M. J. Doktycz, C. J. Sullivan, P. R. Hoyt, D. A. Pelletier, S. Wu and D. P. Allison, *Ultramicroscopy*, 2003, **97**, 209–216.
- 60 S. Kasas, B. Fellya and R. Cargnello, *Surf. Interface Anal.*, 2004, **21**, 400–401.
- 61 M. Kolari, U. Schmidt, E. Kuismanen and M. S. Saliknoja-Salonen, *J. Bacteriol.*, 2002, **184**, 2473–2480.
- 62 M. E. Nuñez, M. O. Martin, P. H. Chand, L. K. Duong, A. R. Sindhurakar and E. M. Spain, *Methods Enzymol.*, 2005, **397**, 256–268.
- 63 S. Sheuring, J. Seguin, S. Marco, D. Levy, B. Robert and J.-L. Rigaud, *Proc. Natl. Acad. Sci. U. S. A.*, 2003, **100**, 1690–1693.
- 64 W. Xu, P. J. Mulhern, B. L. Blackford, M. H. Jericho, M. Firter and T. J. Beveridge, *J. Bacteriol.*, 1996, **178**, 3106–3112.
- 65 X. Yao, M. Jericho, D. Pink and T. Beveridge, *J. Bacteriol.*, 1999, **181**, 6865–6875.
- 66 M. Arnoldi, C. M. Kacher, E. Bauerlein, M. Radmacher and M. Fritz, *J. Appl. Phys.*, 1998, **66**, S613–S617.
- 67 M. Arnoldi, M. Fritz, E. Bauerlein, M. Radmacher, E. Sackmann and A. Boulbitch, *Phys. Rev. E: Stat. Phys., Plasmas, Fluids, Relat. Interdiscip. Top.*, 2000, **62**, 1034–1044.
- 68 S. B. Velegol and B. Logan, *Langmuir*, 2002, **18**, 5256–5262.
- 69 V. Vadillo-Rodriguez, T. J. Beveridge and J. R. Dutcher, *J. Bacteriol.*, 2008, **190**, 4225–4232.
- 70 V. Vadillo-Rodriguez, S. R. Schooling and J. R. Dutcher, *J. Bacteriol.*, 2009, **191**, 5518–5525.
- 71 V. Vadillo-Rodriguez and J. R. Dutcher, *Soft Matter*, 2009, **5**, 5012–5019.
- 72 I. Penegar, C. Toque, S. D. A. Connell, J. R. Smith and S. A. Campbell, in *10th Congress on Marine Corrosion and Fouling*, ed. J. A. Lewis, 1999, pp. 5–15.
- 73 X. Yao, J. Walter, S. Burker, S. Stewart, M. H. Jericho, D. Pink, R. Hunter and T. J. Beveridge, *Colloids Surf., B*, 2002, **23**, 213–230.
- 74 F. Gaboriaud, S. Bailet, E. Dague and F. Jorand, *J. Bacteriol.*, 2005, **187**, 3864–3868.
- 75 M. A. Beckmann, S. Venkataraman, M. J. Doktycz, J. P. Navarro, C. J. Sullivan, J. L. Morrel-Falvey and D. P. Allison, *Ultramicroscopy*, 2006, **106**, 695–702.
- 76 J. Holzer, I. Kampen and A. Kwade, *PARTEC Congress*, 2007.
- 77 F. Gaboriaud, B. S. Parcha, M. L. Gee, J. A. Holden and R. A. Strugnell, *Colloids Surf., B*, 2008, **62**, 206–213.
- 78 F. Gaboriaud, M. L. Gee, R. Strugnell and J. F. L. Duval, *Langmuir*, 2008, **24**, 10988–10995.
- 79 P. Eaton, J. C. Fernandez, E. Pereira, M. E. Pintado and F. X. Malcata, *Ultramicroscopy*, 2008, **108**, 1128–1134.
- 80 A. Cerf, J.-C. Cau, C. Vieu and E. Dague, *Langmuir*, 2009, **25**, 5731–5736.
- 81 P. Schar-Zammaretti and J. Ubbink, *Biophys. J.*, 2003, **85**, 4076–4092.
- 82 G. Francius, O. Domech, M. P. Mingeot-Leclercq and Y. F. Dufresne, *J. Bacteriol.*, 2008, **190**, 7904–7909.
- 83 A. Boulbitch, *J. Electron Microsc.*, 2000, **49**, 459–462.
- 84 E. Dintwa, E. Tijskens and H. Ramon, *Granular Matter*, 2007, **10**, 209–221.
- 85 C. J. Wright and I. Armstrong, *Surf. Interface Anal.*, 2006, **38**, 1419–1428.
- 86 A. L. Koch, *Bacterial Growth and Form*, Kluwer Academic Publishers, Dordrecht, The Netherlands, 2nd edn, 2001.
- 87 V. Norris, J. A. Ayala and K. Begg, et al., *J. Theor. Biol.*, 1994, **168**, 227–230.